

AD-A049 063

NAVAL RESEARCH LAB WASHINGTON D C
A PHASED ARRAY MAINTENANCE MONITORING SYSTEM. PART I.(U)
SEP 77 J K HSIAO, J P SHELTON

F/G 9/5

UNCLASSIFIED

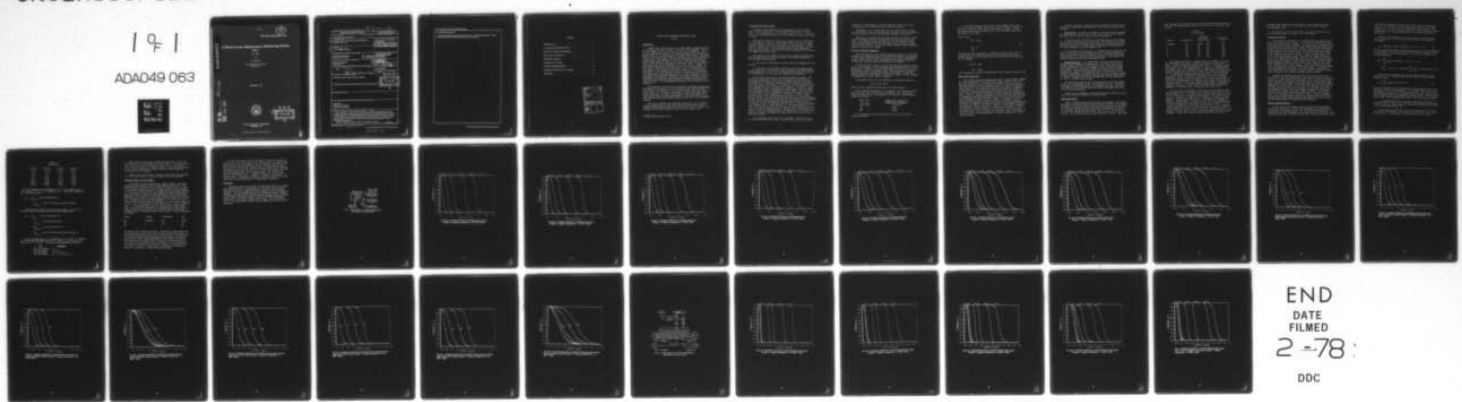
NRL-MR-3613

SBIE-AD-E000 049

DOT-FA-75WAI-556
NL

191

ADA049 063



END
DATE
FILMED
2-78
DDC

12

NRL Memorandum Report 3613

AD A 0 4 9 0 6 3

A Phased Array Maintenance Monitoring System

Part I

J. K. HSIAO

and

J. P. SHELTON

*Target Characteristics Branch
Radar Division*

September 1977

Adc 000049

AD No. _____

DDC FILE COPY



DDC
RECEIVED
JAN 30 1978
B

NAVAL RESEARCH LABORATORY
Washington, D.C.

9 Interim rept.

SECURITY CLASSIFICATION OF THIS PAGE (When Data Entered)

REPORT DOCUMENTATION PAGE		READ INSTRUCTIONS BEFORE COMPLETING FORM
1. REPORT NUMBER NRL Memorandum Report 3613	2. GOVT ACCESSION NO.	3. RECIPIENT'S CATALOG NUMBER
4. TITLE (and Subtitle) A PHASED ARRAY MAINTENANCE MONITORING SYSTEM - PART I	5. TYPE OF REPORT & PERIOD COVERED Interim report on a continuing NRL problem.	
7. AUTHOR(S) J.K./Hsiao J.P./Shelton	6. PERFORMING ORG. REPORT NUMBER 14 NRL-MR-3613	
9. PERFORMING ORGANIZATION NAME AND ADDRESS Naval Research Laboratory Washington, D.C. 20375	8. CONTRACT OR GRANT NUMBER(S)	
11. CONTROLLING OFFICE NAME AND ADDRESS DOT/FAA/MLS Office Washington, D.C.	10. PROGRAM ELEMENT, PROJECT, TASK AREA & WORK UNIT NUMBERS 15 DOT - NRL Problem R12-19 FA-75WAI-556	
14. MONITORING AGENCY NAME & ADDRESS (if different from Controlling Office) 18 SBIE 19 AD-E000 049	12. REPORT DATE 11 September 77	
16. DISTRIBUTION STATEMENT (of this Report) Approved for public release; distribution unlimited.	13. NUMBER OF PAGES 27 1238 p.	
17. DISTRIBUTION STATEMENT (of the abstract entered in Block 20, if different from Report)	15. SECURITY CLASS. (of this report) UNCLASSIFIED	
18. SUPPLEMENTARY NOTES	15a. DECLASSIFICATION/DOWNGRADING SCHEDULE	
19. KEY WORDS (Continue on reverse side if necessary and identify by block number) Phased array Phased array monitoring Phased array maintenance	DDC RECEIVED JAN 30 1978 B	
20. ABSTRACT (Continue on reverse side if necessary and identify by block number) Two methods are described for detecting failures in a phased array through the use of an integral r-f maintenance monitor system. Both methods use an r-f sampling manifold located at the radiating aperture. The methods represented are not exhaustive and are intended as examples. The first method, the balanced monitoring system, requires an adjustment network for zeroing the initial reading, while the second method, Fourier transform system, requires a Fourier transformation computation. Results of computer simulation of these two methods are presented. (continues)		

DD FORM 1473 1 JAN 73

EDITION OF 1 NOV 65 IS OBSOLETE
S/N 0102-014-6601

SECURITY CLASSIFICATION OF THIS PAGE (When Data Entered)

251950 B

20. ABSTRACT (Continued)

This is the first part of this report which treats only a conventional phased array. An array using COMPACT network will be discussed in part 2 of this report.



SECRET
REF ID: A66000

CONTENTS

INTRODUCTION 1
A BALANCED MONITORING SYSTEM 2
DESIGN OF DETECTION THRESHOLDS 3
MONTE CARLO SIMULATION 4
SIMULATION RESULTS 5
LOCATION OF FAILURES 7
FOURIER TRANSFORM METHOD 7
SIMULATED RESULTS FOR FFT METHOD 10
CONCLUSION 11

ACCESSION for	
NTIS	White Section <input checked="" type="checkbox"/>
DDC	Buff Section <input type="checkbox"/>
UNANNOUNCED	<input type="checkbox"/>
JUSTIFICATION _____	
BY _____	
DISTRIBUTION/AVAILABILITY CODES	
Dist.	AVAIL. and/or SPECIAL
A	

A PHASED ARRAY MAINTENANCE MONITORING SYSTEM

PART I

INTRODUCTION

A phased array system consists of a large number of identical radiating elements and phase shifters. Because of this redundancy, failures of a few elements have little effect on the array performance. This graceful degradation feature is a primary advantage of the phased array. Nevertheless, it is often desirable to monitor the operating characteristics of a system to ensure that an acceptably high level of performance is maintained. Furthermore, one would be interested to know when an element breaks down and where it is located. This defective element hence can be replaced at the earliest convenient time, and the array can be maintained at a high performance level at all times. A number of monitoring techniques are applicable to any phased array antenna: the input power to the array can be measured, as can the radiated power. The operation of the phase shifter drive circuits can be continuously monitored. An r-f monitoring system which can detect any failure from the transmitter to the radiating array has a clear advantage over systems which perform indirect monitoring of component operation. With the development of limited scan techniques, feed networks may become more complicated and, although passive networks are highly reliable and not prone to failure, it is nevertheless reassuring to know that they can be monitored.

The objective of this paper is to describe the design and predicted performance of an integral r-f fault-isolation monitoring technique which will indicate and localize any r-f out-of-tolerance condition in the phased array. In this paper, two methods to achieve such array monitoring are described. In both of these methods, monitoring samples are taken directly from the radiating elements. They hence detect all possible failures which might develop along the feed path to the radiating elements.

This type of technique was originally proposed for the U.S Federal Aviation Administration's (FAA) Time Reference Scanning Beam (TRSB), Microwave Landing System (MLS) which uses a linear array. However, this technique can be easily extended to the case of a planar array.

Manuscript submitted September 13, 1977.

A BALANCED MONITORING SYSTEM

A balanced array monitoring system compares two sample outputs taken from two symmetrically located radiating elements in a linear array. A block diagram of such a system is shown in Fig. 1. This system can be operated satisfactorily in the presence of several uncorrected failures.

The monitor operates off-line and an initial state is achieved in the following way: First, the array phase shifters are set to provide a desired radiation pattern. This pattern may be collimated in some specific direction or it may be essentially omnidirectional. In addition, the overall level of the radiation pattern can be reduced by inserting an adjustable attenuator in the main transmission line between the transmitter and the array.

The output of each radiator in the array is sampled and these signals are combined with a manifold network. The manifold network has the following characteristics:

1. The network is matched at all ports, and the sampling ports are isolated.
2. The phase of the transfer coefficient from the sampling ports to the output ports, including the phase settings of the phase shifters, are antisymmetric - that is, the net phase through elements located on the opposite points of the array are different by 180 degrees.

At this point the output of the manifold network is ideally zero. The vector contributions through all the elements of the array are theoretically adjusted to add to zero. However, amplitude and phase variations due to tolerances, temperature variations and the like will cause this output to be nonzero. In addition, a failure anywhere in the array antenna will cause the output to be nonzero. Therefore, a separate transmission line is included which couples energy from the transmitter output and adds to the manifold output signal. Phase and amplitude adjustments in the transmission line allow the detected output to be set to zero. This is achieved by a feedback loop shown in Fig. 1. Initially switch 1 is closed and switch 2 is open. An error signal which is derived from the difference between the signal from the manifold and that of the transmitter is fed back to a gain control device G which in turn adjusts both the amplitude and phase of the signal from the transmitter. This will eventually set the input to the detection device at a quiescent state. After this switch 2 is closed and switch 1 is open. The control network will then cycle the phase shifter states one pair at a time as discussed earlier. Whenever an out-of-tolerance condition is detected, correlation with the information in the control network can be used to determine which phase shifter and which bit has suffered a failure.

The philosophy of operation that is adopted at this point is to set up the test procedure so that a nonzero output indicates a failed

condition. In this manner it will be possible to detect the failure by measuring only the amplitude output from the detector.

Furthermore, it is required only that the array exhibit internal self consistency - that is, the amplitude and phase of all the radiators should be consistent as the various phase settings are exercised.

Therefore, it is specified that phase shifters are tested in pairs located at opposite points in the right half and the left half of the array. Both these two phase shifters are cycled through 360 degrees. If both phase shifters and their feed network have no failure, a zero output will be observed. On the other hand, a nonzero output represents failure in this pair of elements.

DESIGN OF DETECTION THRESHOLDS

Since the purpose of the integral performance monitor is to detect failures in the array antenna, it is necessary to estimate the amplitudes of the signals produced by these failures at the output of the monitor system. This is done by first establishing the minimum allowable out-of-tolerance conditions which are required to be detected.

If four-bit phase shifters are used, the minimum detectable failure will be 22.5 degrees, so that the system must alarm when there is a 22.5 degree error. However, the cumulative allowable tolerance for each element channel is about 10 degrees. Thus, one encounters the classical detection problem of setting the threshold low enough to detect the desired signals but high enough to avoid false alarms. In this instance, a threshold can be set at about 15 degrees.

If the phase error is ϕ , the amplitude of the monitor output is

$$E_{\phi} = 2E_0 \sin (\phi/2)$$

where E_0 is the amplitude contributed by one phase shifter.

For an angle-error threshold of 15 degrees, the amplitude threshold must be set at .26E or about -11.67 dB relative to E_0 . The signal levels for phase errors corresponding to the bits of a four-bit phase shifter are listed:

<u>Phase Error</u>	<u>Signal level relative to threshold at 15 degrees</u>
22.5 (deg)	3.49 (dB)
45	9.34
90	14.68
180	17.69

It is clear that the larger and more serious phase errors are readily detectable.

If an amplitude error exists in one of the elements and is the same for all phase settings, then this error will produce a signal output from the monitor as the phase of the element is cycled. If the amplitude of the element is given by $E_0 + \Delta E$, the maximum signal from the monitor will be $2\Delta E$.

Thus, we have

$$2\Delta E = .26E_0 \tag{1}$$

$$\frac{\Delta E}{E_0} = .13$$

This amplitude error represents a tolerance of about one dB. If it is required that the threshold be exceeded for one-half of the phase-shifter settings, as will likely be the case for phase-error detection, Eq. (1) becomes

$$1.414\Delta E = .26E_0$$

$$\Delta E = .1838,$$

and the amplitude tolerance corresponding to this signal is about 1.5 dB.

MONTE CARLO SIMULATION

The previous analysis indicates that there is enough signal strength for failure detection in this monitoring system. However, due to the fact that variations of the phase and the amplitude at the output of radiating elements caused by component tolerance, temperature change and other factors, cannot be described precisely, they must be treated as random variables. It would be interesting to estimate the probability of detection and false alarm when these system errors are assumed to have certain statistical distribution and when a detection threshold is given. This is a classical problem of test of hypothesis which amounts to finding the conditional probability distribution of the manifold output level given the condition that a failure is present, or the conditional probability that a failure is absent. Estimation of such a probability distribution is difficult, because the joint probability of the effect of component tolerance, variation of environmental conditions and measurement noise is not known. However, a Monte Carlo simulation performed by a digital computer can yield enough information to predict the performance of such a system. In particular, when the required false alarm rate (10^{-2}) and detection probability range (.99) are modest as in this case, a not-too-large set of simulated samples will yield adequate results.

In order to achieve a simulation with acceptable results, the following basic assumptions concerning the failure modes and system errors are made.

Failure Mode. Two types of failures are simulated in this program. The first type is a failure which occurs in the phase shifter network. The second type is one that occurs in the feed network.

In the first type of failure, it is assumed that the phase shifter bit is either stuck-to-zero or stuck-to-one. For example, in a system which has 4-bit phase shifters, if the first bit is stuck-to-zero, then the phase setting of 22.5 degrees will be mistaken as 0 degrees while 67.5 as 45 degrees, 112.5 as 90 degrees, etc.

In the second type of failure, it is assumed that the amplitude and phase of the output from the antenna may have a constant biased error. This may happen when the feed network of one of the elements develops failures and causes a shift in amplitude and phase of the output, even though the phase shifter operates satisfactorily.

Error Assumption. It is assumed that the phase shifter and its feed network are subject to random errors. Two types of errors are assumed, namely amplitude error and phase error. Since these errors may be contributed to by a large number of sources, based on central limit theory, it is reasonable to assume that they may have a normal distribution. However, the random variables of these errors are not stochastic processes. In other words, they are not a function of time. Within a single sampling exercise, they may vary from one phase setting to another. However, they remain unchanged when several measurements are made on a single phase setting.

The second type of error may be contributed by the system random noise, such as measurement noise, shot-noise and the like. This noise is assumed to be Rayleigh and it is a stochastic process. The noise level may vary at each measurement when several measurements are made on the same phase setting.

Based on these assumptions, simulations have been carried out, and some of the results are shown in the next section.

SIMULATION RESULTS

Figs. 2a through 2h show the probability distribution of the manifold output levels where phase shifter bits have failures. The standard deviation of the phase shifter phase and amplitude errors and the signal to noise ratio assumed in these simulations are summarized in Table 1. It is evident that the manifold output level for a failure in the 1st bit (the least significant bit) is very close to that of the case of no failure. It is this case which is most difficult to detect. This table

also includes the threshold level for a 90 percent detection probability with the corresponding false alarm rate for the case of a failure in the 1st bit.

Table 1
False Alarm Rate

σ (phase)	σ (amplitude)	Threshold (90 percent SNR detection)	False Alarm Rate
2 degrees	.05	20 dB .275	.07
4	.05	20 .35	.18
2	.10	20 .28	.16
4	.10	20 .27	.26
6	.15	20 .19	.55
8	.20	20 .18	.68
4	.10	15 .22	.62
4	.10	10 .23	.83

The standard deviation σ of phase error is in degrees. For a normal distribution, more than 99 percent of samples lie within the 3σ point. Usually the maximum allowable phase error is about half of the phase angle of the least significant bit. Thus a $\sigma = 4$ degrees would be a typical case. The amplitude error is measured in percent of the amplitude of the power transmitted to the phase shifter in an ideal case which is assumed to be unit. For a typical case, one may assume that $\sigma = .1$ which gives a maximum amplitude error $\pm .3$. For this typical case with an SNR of 20 dB, when a threshold of 90 percent detection probability is used, a modest .26 false alarm rate can be achieved. If phase error amplitude error and signal to noise ratio increase beyond this point the false alarm rate increases very rapidly, as one may conclude from Table I. The results showed in this table are intended as examples. Certainly, if one chooses a different level of detection probability, one could achieve a different false alarm rate.

Fig. 3a shows the probability distribution of the manifold output when the amplitude of one element has a constant biased error of 25, 50 and 75 percent. Fig. 4a shows the cases of constant biased phase angle errors of 20 degrees, 40 degrees and 60 degrees. These errors may be caused by failure in r-f power source, transmission network and phase shifters. In both these two plots, it is assumed that σ (phase) = 4 degrees, σ (amplitude) = .1 and SNR = 20 dB. If the same threshold of the case having the same phase error and amplitude in Table I is used, a detection probability of .58 would be achieved for a worst case of a constant amplitude error of 25 percent while a .8 detection probability can be achieved for a worst case of a constant biased phase error of 20 degrees. In both cases, the false alarm rate remains the same as shown in Table 1. Figs. 3b, 3c and 3d show the manifold output level for

constant biased amplitude error at different phase, amplitude errors and SNR levels. Figs. 4b, 4c and 4d are for the cases of constant biased phased error.

One should notice due to the effect of initial zeroing, insertion phase variation cannot be checked out by this method.

LOCATION OF FAILURES

In the previous discussions, it is assumed that the radiating elements are tested a pair at a time. It is therefore impossible to tell which one of the pair has a failure. In this section, an algorithm will be described which allows location of the element which may have a stuck-to-one or a stuck-to-zero failure. This is illustrated by an example. Assume that the system under test has 4-bit shifters, and the first bit of the element in the left half array is stuck-to-one and the element in the right half array has no failure. Further, assume that at this point of the test procedure, both left element and right element are set to the 0 degree phase setting. Since the left element is actually set at 22.5, an output will be observed which indicates a failure exists between these two elements. Now, suppose that we hold the left element phase unchanged and vary the phase of the right element to +22.5 and -22.5, one sees while at 22.5 degrees, the output becomes zero and at -22.5, the output is increased. On the other hand, if the right element is held unchanged while the phase of the left element is switched to +22.5 degrees and -22.5 degrees, one would observe no change of output level. For these tests, the faulty element may be located.

Although this example shows only the case of the failure of the first bit of a four bit phase shifter, this same approach can apply to any bit in a phase shifter with any number of bits as long as the monitor system can detect the failure in the first place. From previous simulation results one can easily distinguish which bit has failed by simply observing the output levels. Hence, this algorithm can be described as follows: When a failure occurs, one flips the suspected bit of one of the elements from zero state to one-state, or vice versa, while holding the phase shifter of the other element unchanged. If the phase shifter of that element has either a stuck-to-zero or a stuck-to-one error, this flipping will not change the output. However, varying the phase state of a normal phase shifter will alternate the output level. Note that the constant biased phase and amplitude errors due to failure of feed network cannot be located by this technique.

FOURIER TRANSFORM METHOD

In this method, the sampled outputs from the radiating elements are fed into the manifold without the antisymmetrical requirements as discussed in the previous method. The array phase shifters are initially set such that a minimum output is observed at the manifold. This output does not have to be zero or near zero. Therefore, the extra feed

line from the transmitter and the control loop for zeroing manifold output is not required. During the monitoring operation, each phase shifter is cycled through all its phase states from 0 degrees to 360 degrees, one at a time. A Fourier transform is then performed on these outputs which may be accomplished either in a digital form or in an analog form.

Outputs from the manifold can be represented as the following equation when one of the phase shifters is cycled from 0 degrees to 360 degrees:

$$f_i = A \exp(j\phi) + a_i \exp [j(2\pi/N)i], \quad i = 0, 1, \dots, N-1, \quad (2)$$

where N is the total number of phase shifter states, a_i is the amplitude of the element output at each phase shifter state, and $A \exp(j\phi)$ is the residual signal in the manifold network. The Fourier transform output can be represented

$$F_k = \sum_{i=0}^{N-1} f_i \exp [-j(2\pi/N)ki], \quad k = 0, 1, \dots, N-1$$

$$= \sum_{i=0}^{N-1} A \exp \left(j[\phi - (2\pi/N)ki] \right) + \sum_{i=0}^{N-1} a_i \exp [-j(2\pi/N)(k-1)i] \quad (3)$$

The first term represents the DC level which is equal to zero except when $k = 0$. Therefore this term is ignored in the following analysis. Hence,

$$F_k = \sum_{i=0}^{N-1} a_i \exp [-j(2\pi/N)(k-1)i] \quad (4)$$

where it is assumed that the phase shifter output remains constant when the phase shifter is being switched. It is evident that in the above expression, F_k is zero for all k , except when $k=1$. This is to say that under normal conditions, all harmonics from the Fourier transform filter are zero except the DC and fundamental component ($k=0,1$). When failure occurs, other higher harmonics will appear. This is shown as follows:

As an example, Table 2 shows the phase state indices of a 4 bit phase shifter. Indices of those phase states having the same phase output are grouped together when a stuck-to-one or stuck-to-zero failure occurs in that phase shifter bit.

In this table the first bit is the least significant bit which in this case is 22.5 degrees. For example, if the first bit has a stuck-to-zero error, all odd indices will be mistaken to be even thus

Table 2
Phase State

<u>1st bit</u>	<u>2nd bit</u>	<u>3rd bit</u>	<u>4th bit</u>
0,1	0,2	0,4	0,8
2,3	1,3	1,5	1,9
4,5	4,6	2,6	2,10
6,7	5,7	3,7	3,11
8,9	8,10	8,12	4,12
10,11	9,11	9,13	5,13
12,13	12,14	10,14	6,14
14,15	13,15	11,15	7,15

$i = 1$ (22.5 degrees) will be mistaken to be $i = 0$ (0 degree) and $i = 3$ (67.5 degrees) to be $i = 2$ (45 degrees), etc. Under this assumption, Eq. (4) can be written:

$$F_k = \sum_{i=0,2,\dots} a \exp[-j(2\pi/N)(k-1)i] + \sum_{i=1,3,\dots} a \exp[-j(2\pi/N)(k-1)i] \exp[-j(2\pi/N)]$$

Both these two terms will be zero except when $k = 1$ and $k = 9$. For the case of the failure of the 2nd bit, one may write:

$$F_k = \sum_{i=0,4,\dots} a \exp[-j(2\pi/N)(k-1)i] + \sum_{i=1,5,\dots} a \exp[-j(2\pi/N)(k-1)i] + \left[\sum_{i=2,6,\dots} a \exp[-j(2\pi/N)(k-1)i] + \sum_{i=3,7,\dots} a \exp[-j(2\pi/N)(k-1)i] \right] \exp[j2(2\pi/N)]$$

It can be shown that $F_k = 0$, except when $k = 1, 5$ and 13 . Similarly, one can show that when the third bit failed, F_k will not be zero, when $k = 3, 7, 11$, and 15 . The results are summarized as follows:

<u>Bit</u>	<u>Harmonics</u>
1st (22.5 degree)	1, 9
2nd (45 degree)	1, 5, 13
3rd (90 degree)	1, 3, 7, 11, 15
4th (180 degree)	2, 4, 6, 8, 10, 12, 14

This property can be used to locate the failed bit. One of the implementations of this approach is shown in Fig. 5. The manifold output is first mixed with r-f signal and formed into I and Q channels which are then converted into digital signals. These digitized signals are then Fourier transformed. Outputs from this Fourier transform filter are used for detection.

However, one can not detect a constant biased phase and amplitude error and the variation of insertion phase by using this method.

SIMULATED RESULTS FOR FFT METHOD

This method has been simulated on a digital computer. The phase shifter is again assumed to have an amplitude and phase error. The distribution of these errors is assumed to be Gaussian as in the case of the balanced monitoring system. A random noise in terms of signal to noise ratio is also assumed. The manifold outputs are recorded when one of the phase shifters is cycled through all possible phase states. A discrete Fourier transform is then performed on this recorded data. Amplitudes of the outputs of the Fourier transform filter are then combined into four groups. Each group represents the failure of a certain bit. For example, outputs of the harmonics 4, 6, 8, 10, 12, 14 are combined into a single output for monitoring the 4th bit while harmonics $k = 3, 7, 11, 15$ are combined for the third bit, etc. This is shown in Fig. 5. In this simulation, only the largest value in each group is used. The probability distribution of the amplitude of this signal is shown in Figs. 6a, 6b, 6c and 6d for different values of phase and amplitude errors at different signal to noise ratio. This is summarized as follows:

Figure	σ (phase)	σ (amplitude)	SNR
6a	2 degrees	.05	20 dB
6b	4	.1	20
6c	6	.15	20
6c	4	.1	10

For each bit, two curves are plotted. The one has a lower output level is for the case of no failure or for the case when other bits have a failure which may affect the output of this bit group. The other curve is for the case when the bit has either a stuck-to-one or a stuck-to-zero failure. These figures indicate that for a signal to noise of more than 20 dB, the output level for the case of the failure of the 1st bit (the worst case) and that of no-failure is so far separated that there is no possibility of false alarm when an appropriate threshold level is chosen. In this aspect, it seems that this method is superior to the method of balance monitoring system.

For the cases shown in Fig. 6a through 6d the output taking from the FFT filter is the amplitude of the complex output. To compute this amplitude value the real component and the imaginary component of this complex output must be squared and summed. The amplitude is equal to the square root of this sum. However, similar results can be formed by replacing the amplitude with the sum of the absolute values of both the real and imaginary parts of the complex output. This reduces the required computational steps. Simulated results for this case are shown in Fig. 7 which has a σ (phase) = 4 degrees, σ (amplitude) = .1 and SNR = 20 dB. Comparing this figure with that of Fig. 6b of a similar case, one sees that there is no appreciable difference.

CONCLUSION

Two methods have been described for detecting failures in a phased array through the use of an integral r-f maintenance monitor system. Both methods use an r-f sampling manifold located at the radiating aperture. The methods presented are not exhaustive and are intended as examples. The first method, the balanced monitoring system, requires an adjustment network for zeroing the initial reading, while the second method, Fourier Transform system, requires a Fourier transformation computation. This report consists of two parts. This is the first part. In the second part an array using a COMPACT feed network will be discussed.

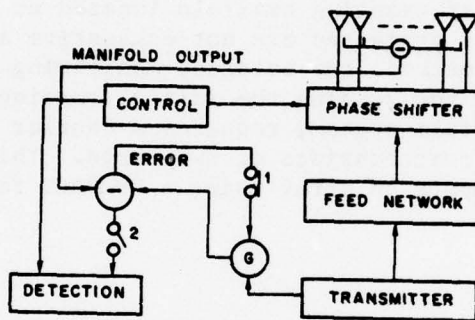


Fig. 1. Block diagram of a balanced phased array maintenance monitoring system

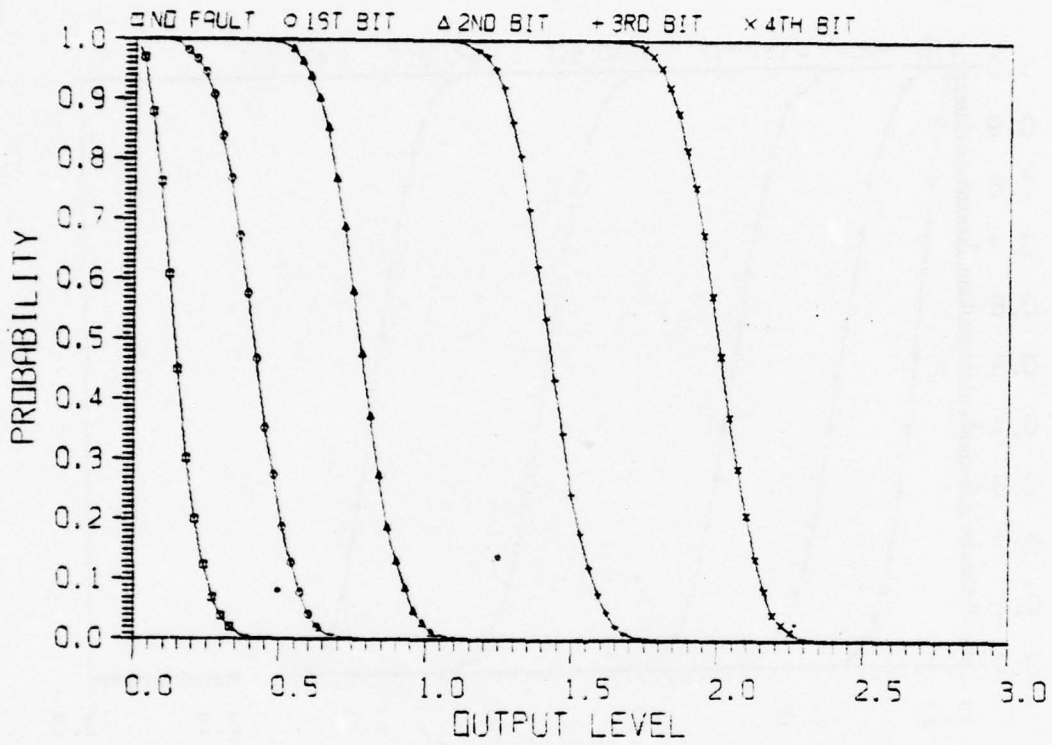


Fig. 2(a) - Probability distribution of manifold output level,
 $\sigma(\text{phase}) = 2$ degrees, $\sigma(\text{amplitude}) = .05$, SNR = 20dB

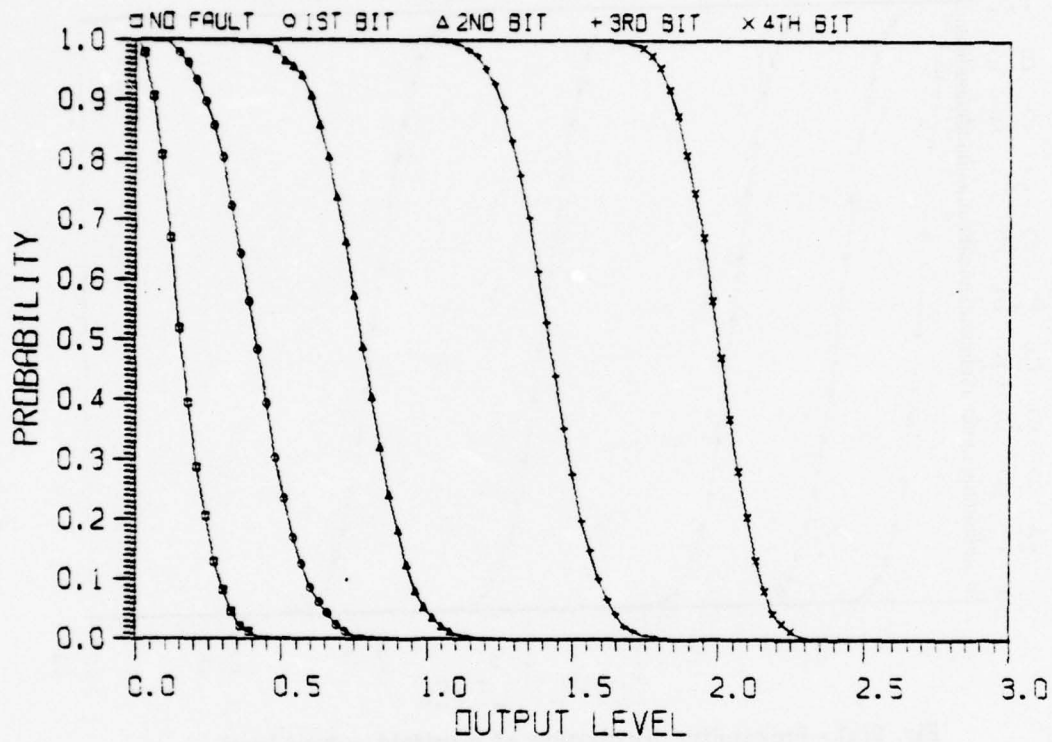


Fig. 2(b) - Probability distribution of manifold output level,
 $\sigma(\text{phase}) = 4$ degrees, $\sigma(\text{amplitude}) = .05$, SNR = 20dB

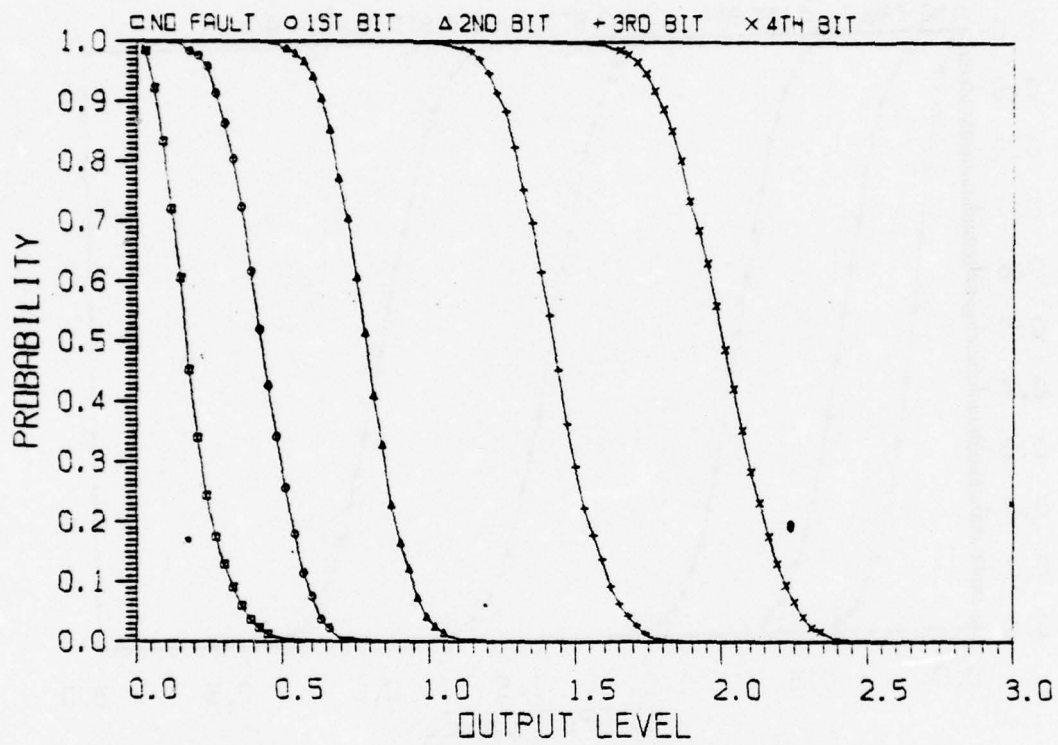


Fig. 2(c) - Probability distribution of manifold output level,
 $\sigma(\text{phase}) = 2$ degrees, $\sigma(\text{amplitude}) = .1$, SNR = 20dB

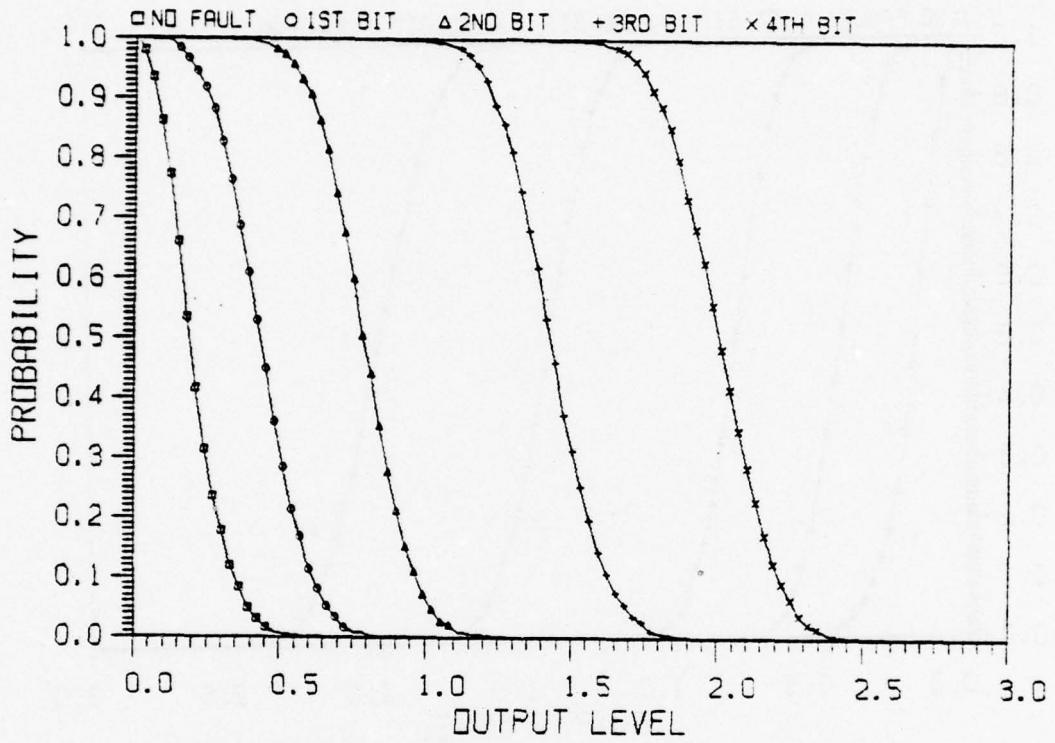


Fig. 2(d) - Probability distribution of manifold output level,
 $\sigma(\text{phase}) = 4$ degrees, $\sigma(\text{amplitude}) = .1$, SNR = 20dB

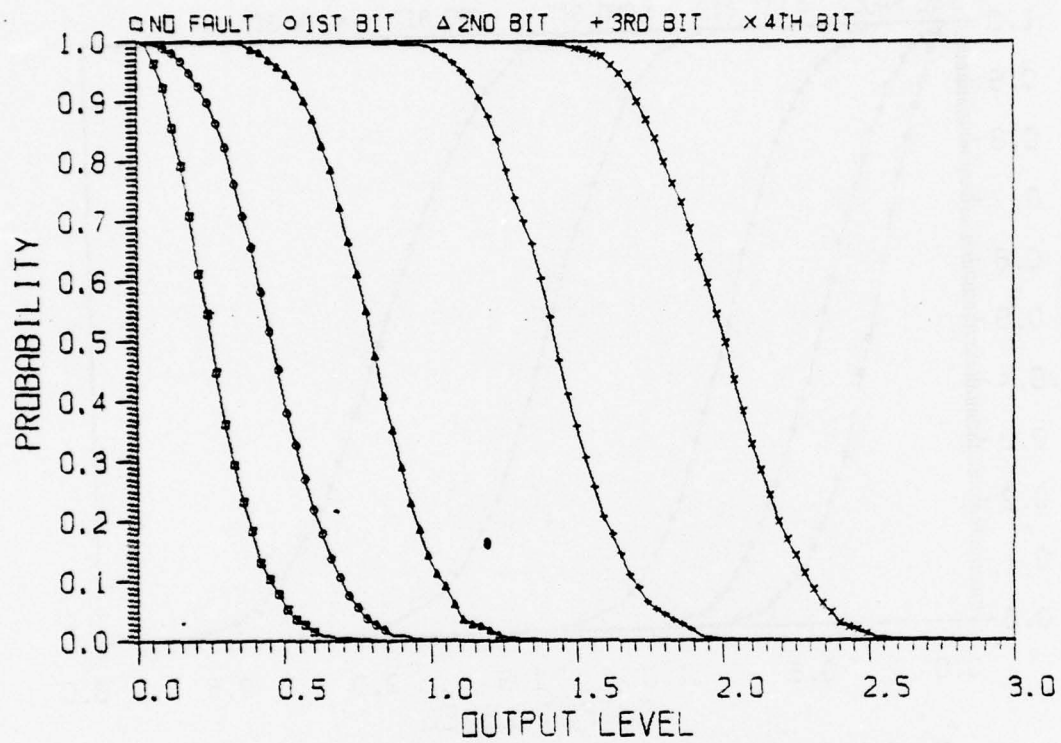


Fig. 2(e) - Probability distribution of manifold output level,
 $\sigma(\text{phase}) = 6$ degrees, $\sigma(\text{amplitude}) = .15$, SNR = 20dB

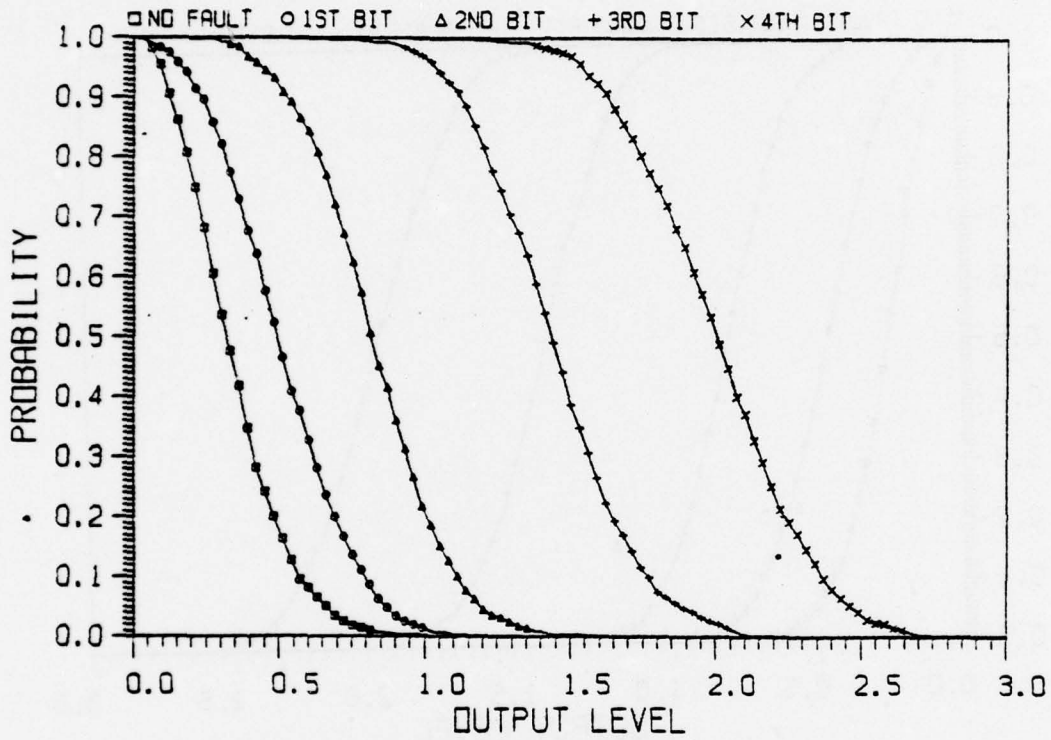


Fig. 2(f) - Probability distribution of manifold output level,
 $\sigma(\text{angle}) = 8$ degrees, $\sigma(\text{amplitude}) = .2$, SNR = 20dB

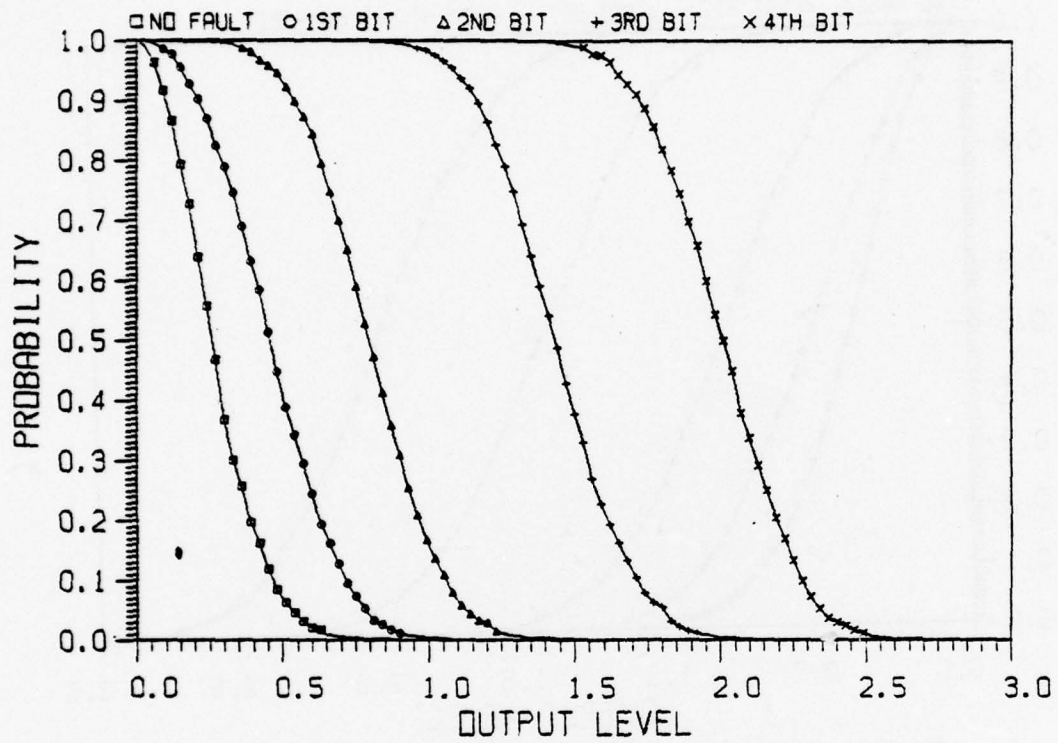


Fig. 2(g) - Probability distribution of manifold output level,
 $\sigma(\text{angle}) = 4$ degrees, $\sigma(\text{amplitude}) = .1$, SNR = 15dB

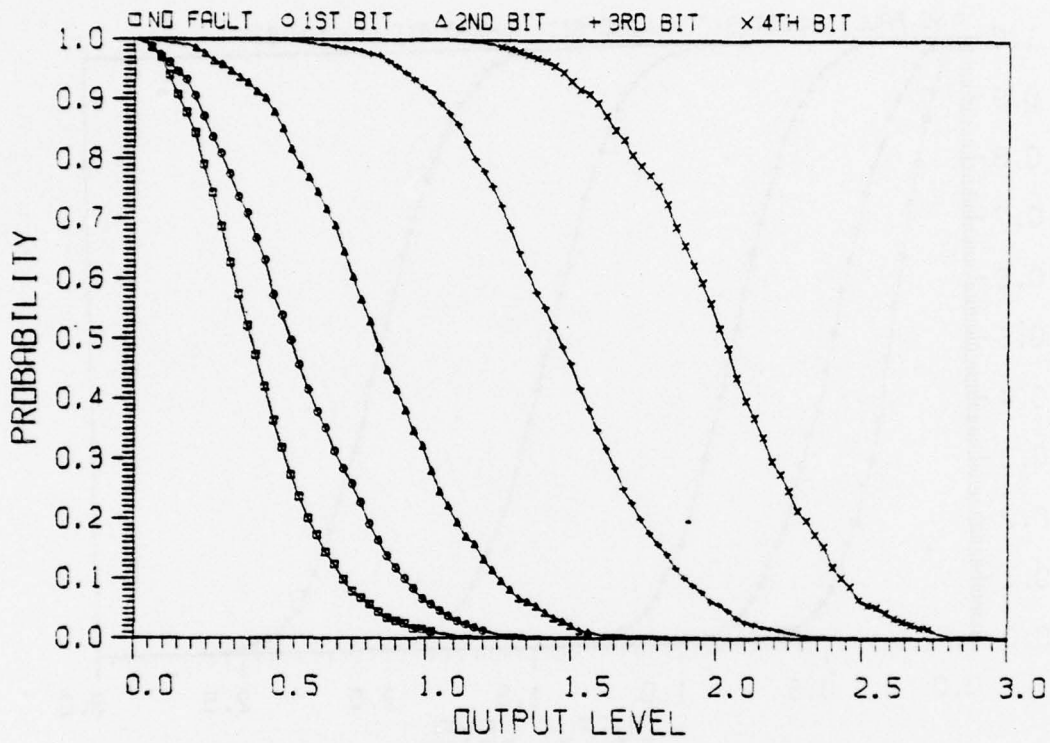


Fig. 2(h) - Probability distribution of manifold output level,
 $\sigma(\text{angle}) = 4$ degrees, $\sigma(\text{amplitude}) = .1$, SNR = 10dB

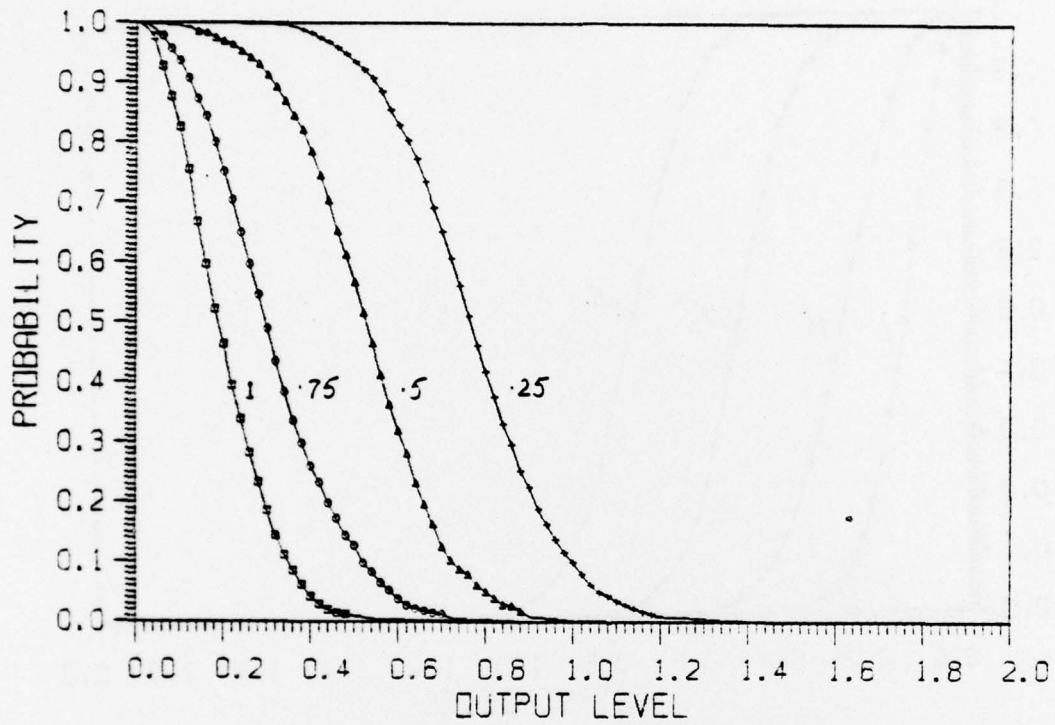


Fig. 3(a) - Probability distribution of manifold output level when one element amplitude is reduced $\sigma(\text{phase}) = 4$ degrees, $\sigma(\text{amplitude}) = .1$, SNR = 20dB

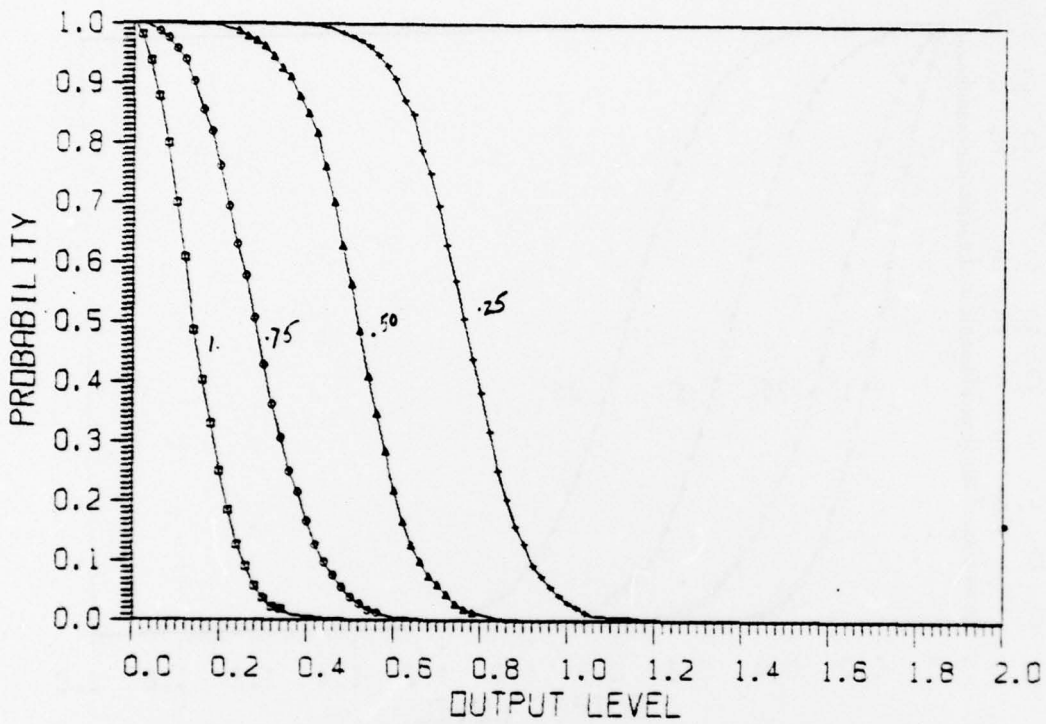


Fig. 3(b) - Probability distribution of manifold output level when one element amplitude is reduced $\sigma(\text{phase}) = 2$ degrees, $\sigma(\text{amplitude}) = .05$, SNR = 20dB

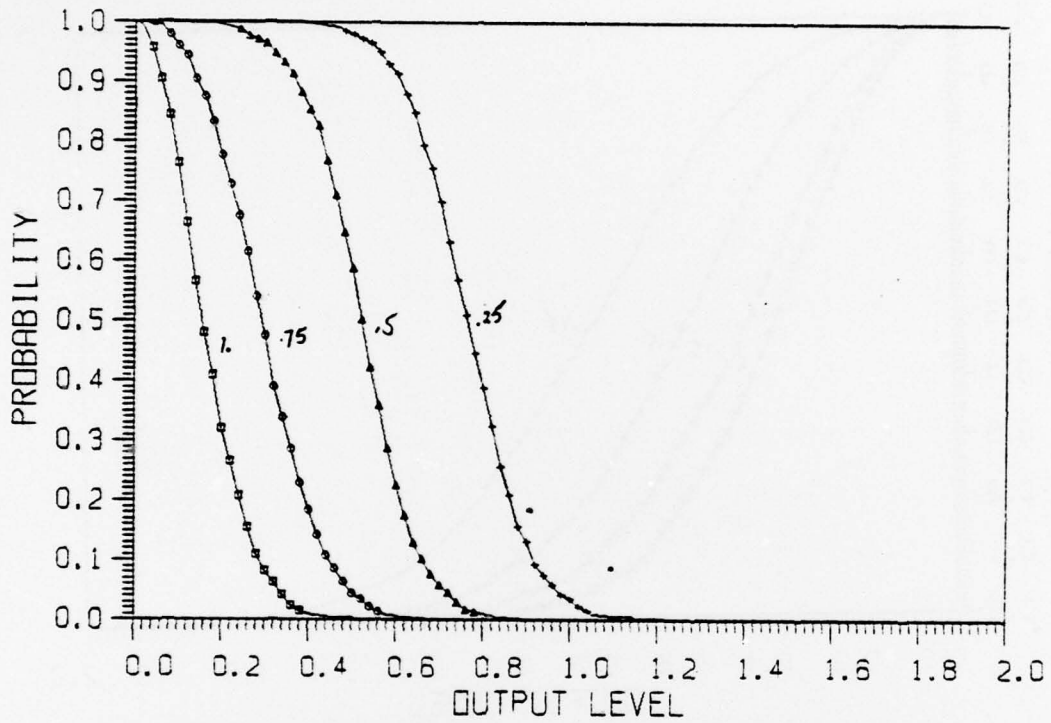


Fig. 3(c) - Probability distribution of manifold output level when one element amplitude is reduced $\sigma(\text{phase}) = 4$ degrees, $\sigma(\text{amplitude}) = .05$, SNR = 20dB

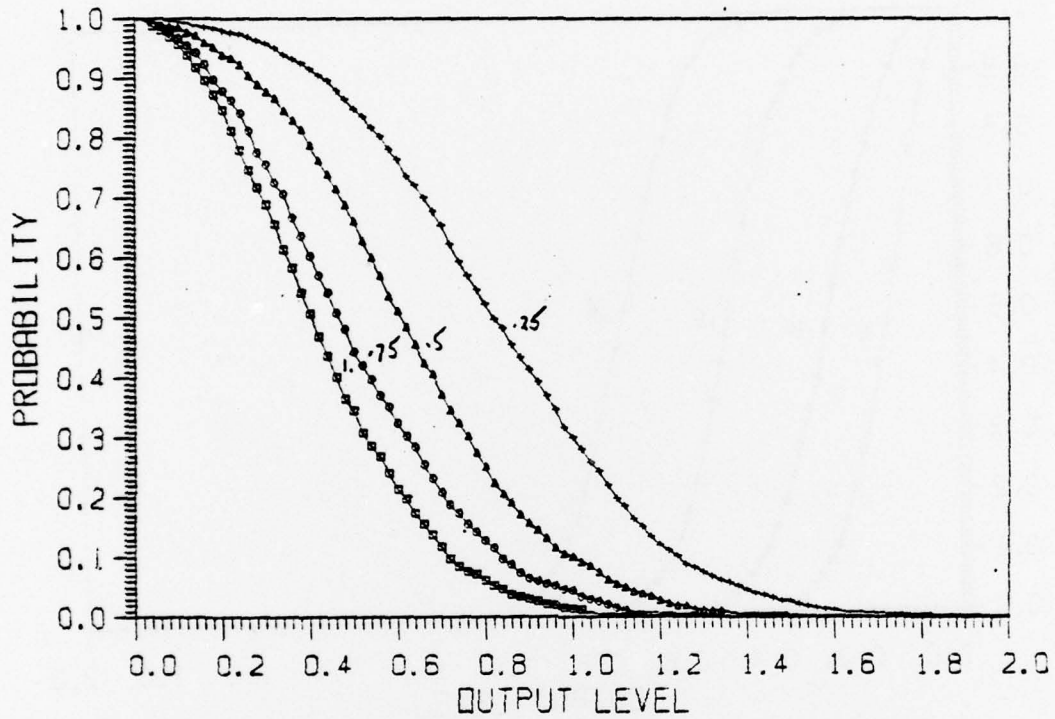


Fig. 3(d) - Probability distribution of manifold output level when one element amplitude is reduced $\sigma(\text{phase}) = 4$ degrees, $\sigma(\text{amplitude}) = .1$, SNR = 10dB

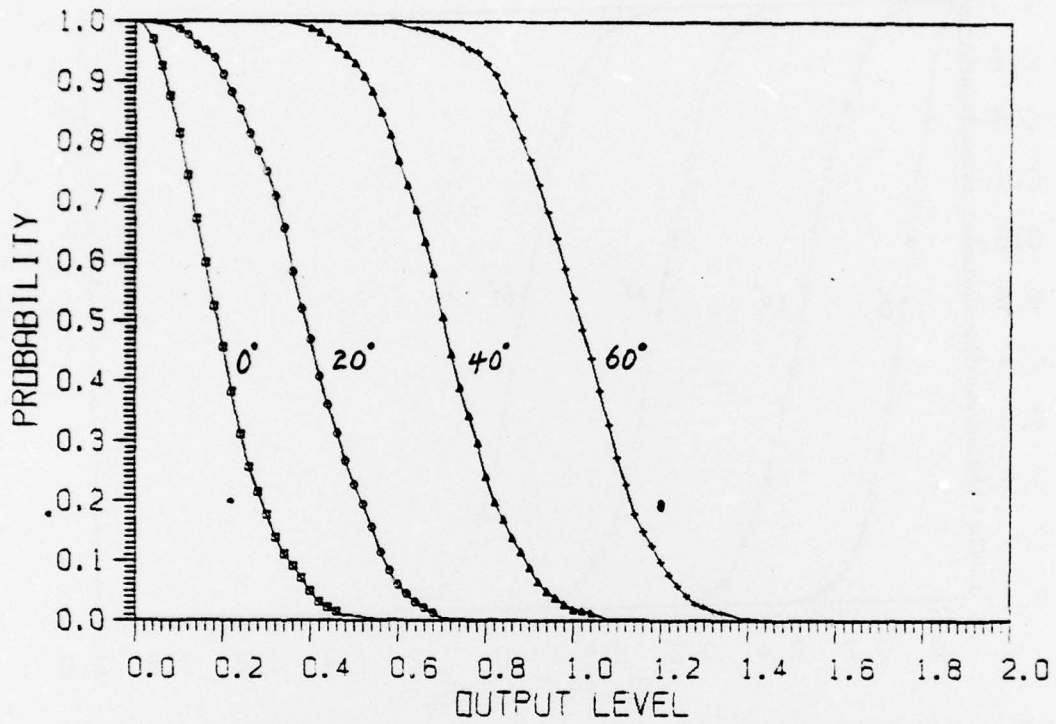


Fig. 4(a) - Probability distribution of manifold output level when constant biased phase error is present $\sigma(\text{phase}) = 4$ degrees, $\sigma(\text{amplitude}) = .1$, SNR = 20dB

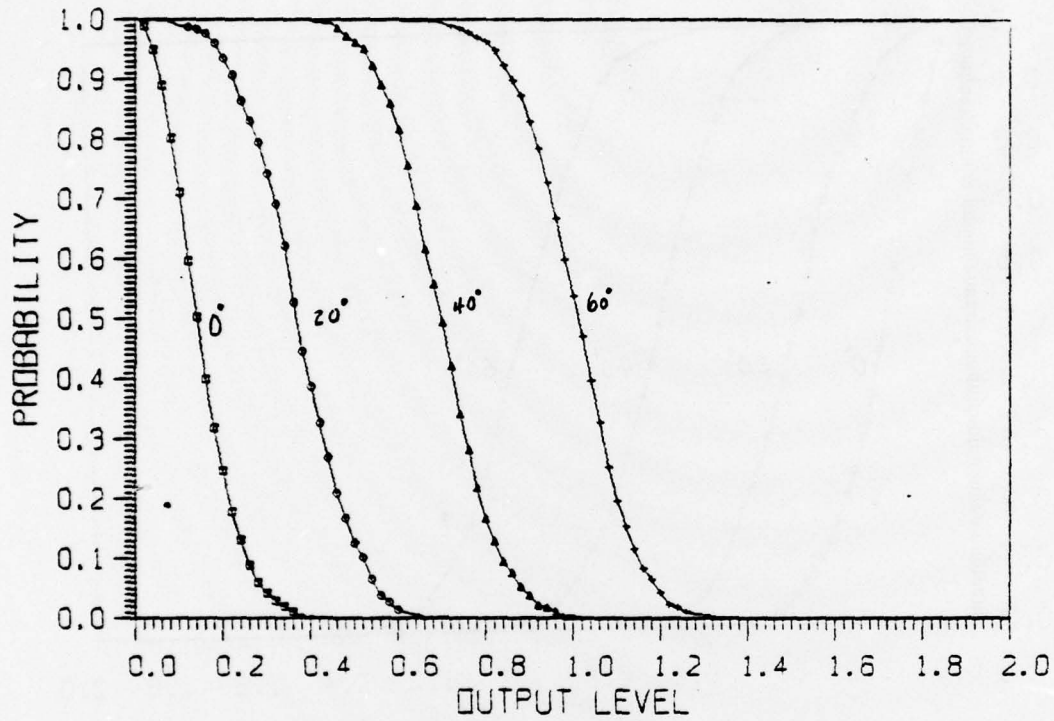


Fig. 4(b) - Probability distribution of manifold output level when constant biased phase error is present $\sigma(\text{phase}) = 2$ degrees, $\sigma(\text{amplitude}) = .05$, SNR = 20dB

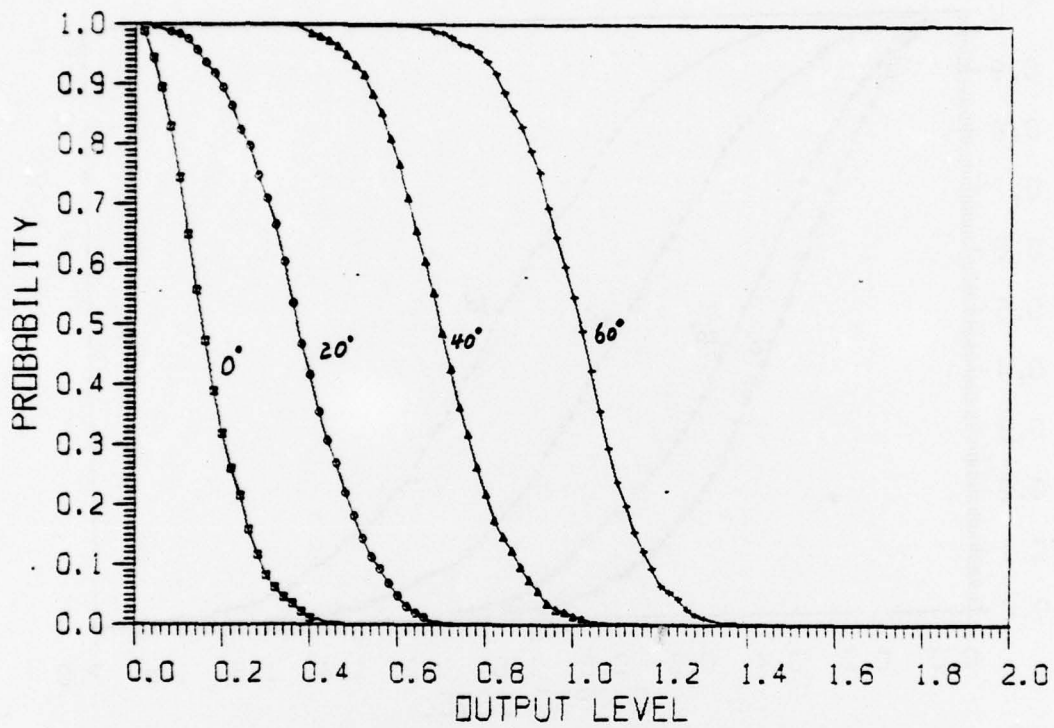


Fig. 4(c) - Probability distribution of manifold output level when constant biased phase error is present $\sigma(\text{phase}) = 4$ degrees, $\sigma(\text{amplitude}) = .05$, SNR = 20dB

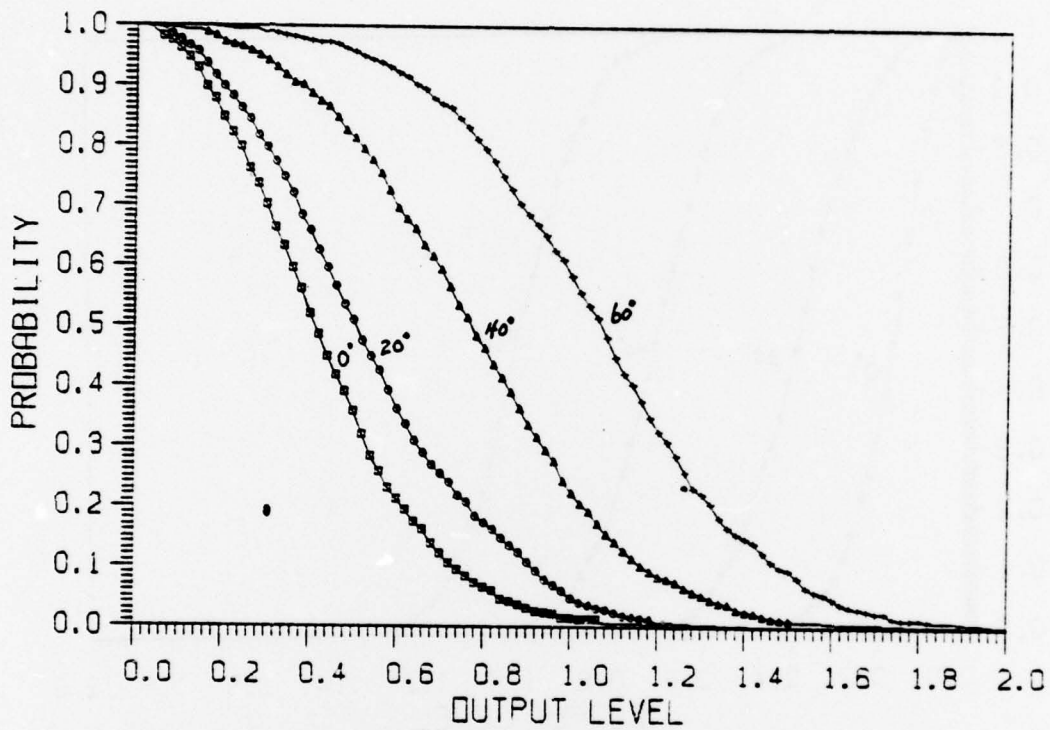


Fig. 4(d) - Probability distribution of manifold output level when constant biased phase error is present $\sigma(\text{phase}) = 4$ degrees, $\sigma(\text{amplitude}) = .1$, SNR = 10dB

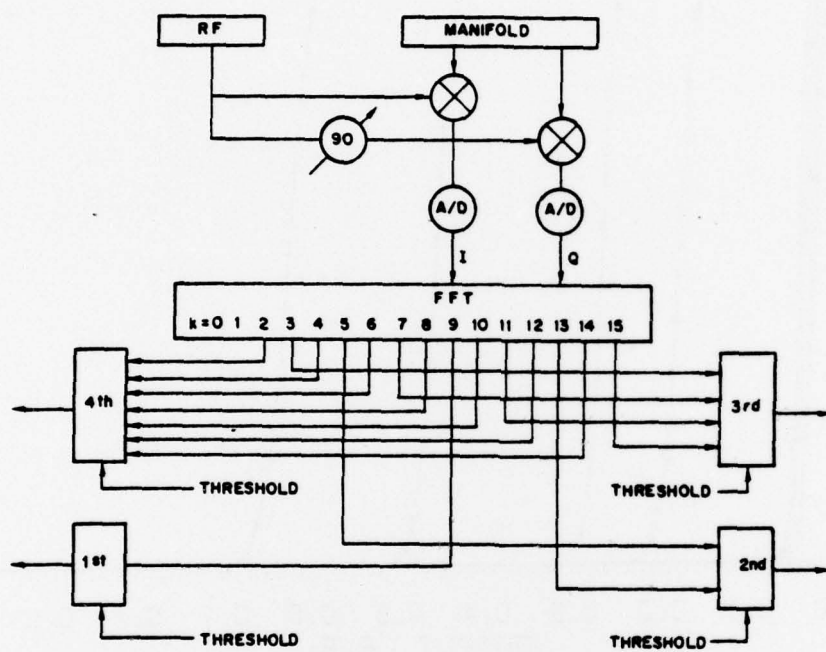


Fig. 5 - A block diagram of a Fourier transform array maintenance monitoring system

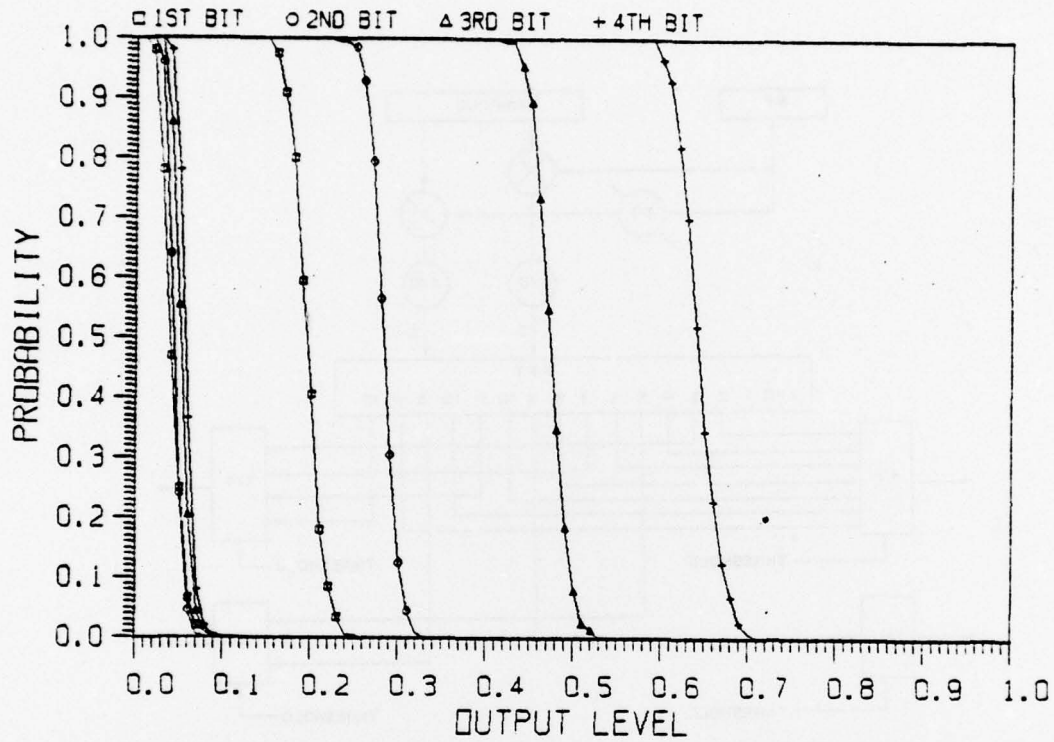


Fig. 6(a) - Probability distribution of Fourier transform filter output
 $\sigma(\text{phase}) = 2$ degrees, $\sigma(\text{amplitude}) = .05$, SNR = 20dB

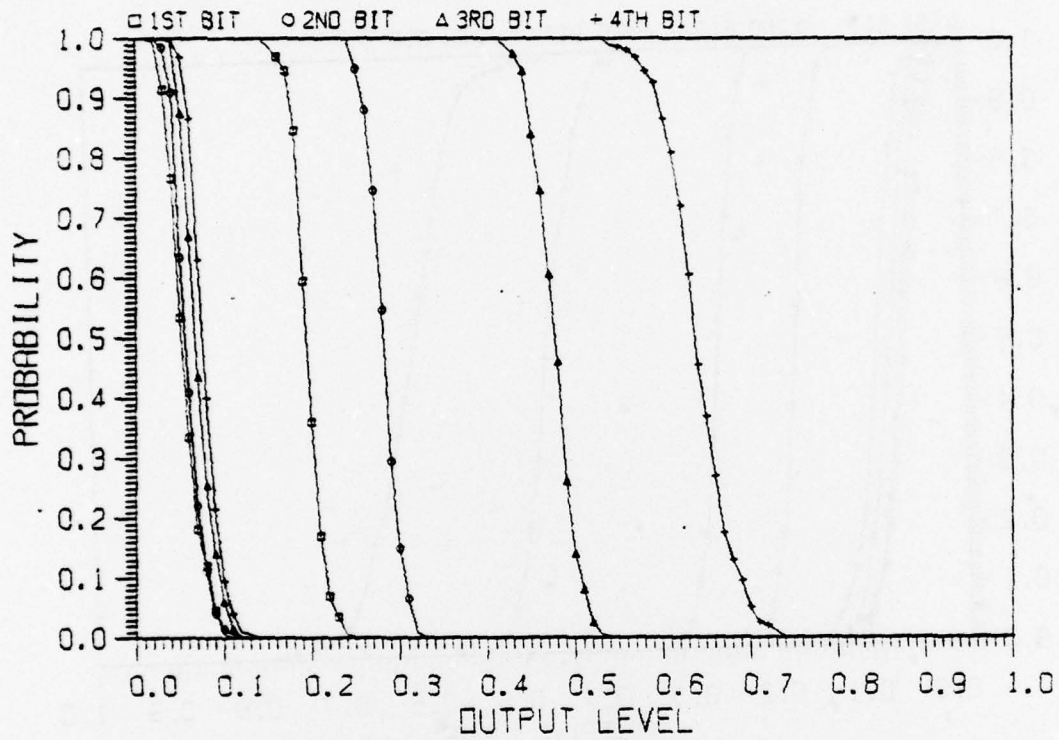


Fig. 6(b) - Probability distribution of Fourier transform filter output
 $\sigma(\text{phase}) = 4$ degrees, $\sigma(\text{amplitude}) = .1$, SNR = 20dB

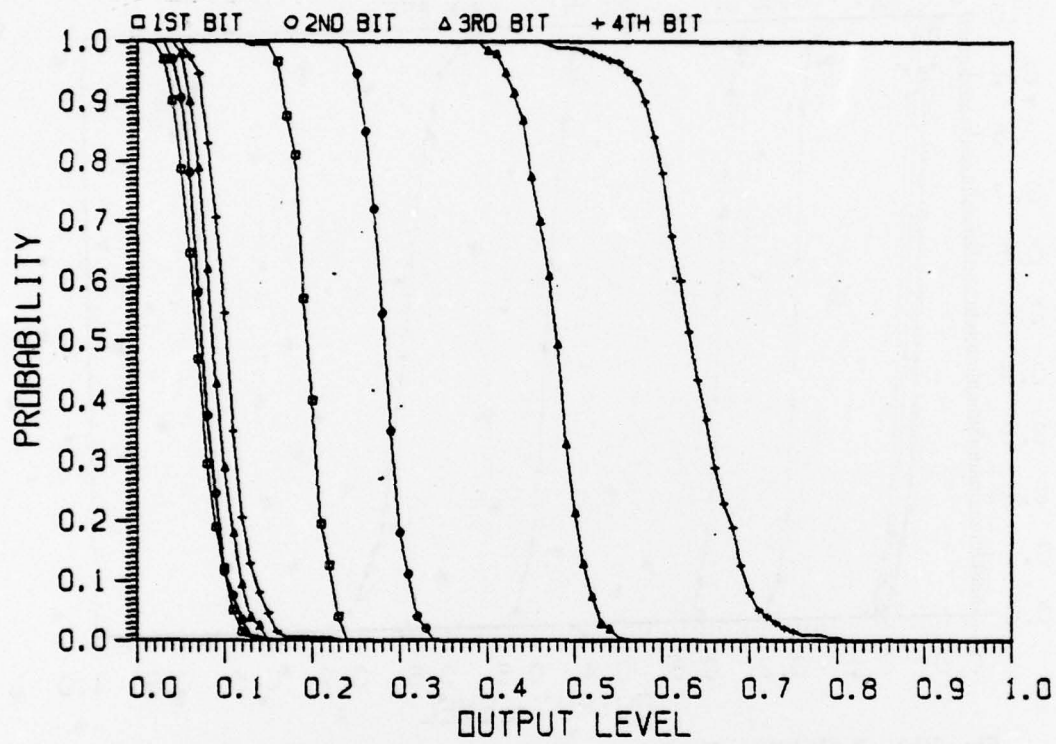


Fig. 6(c) - Probability distribution of Fourier transform filter output
 $\sigma(\text{phase}) = 6$ degrees, $\sigma(\text{amplitude}) = .15$, SNR = 20dB

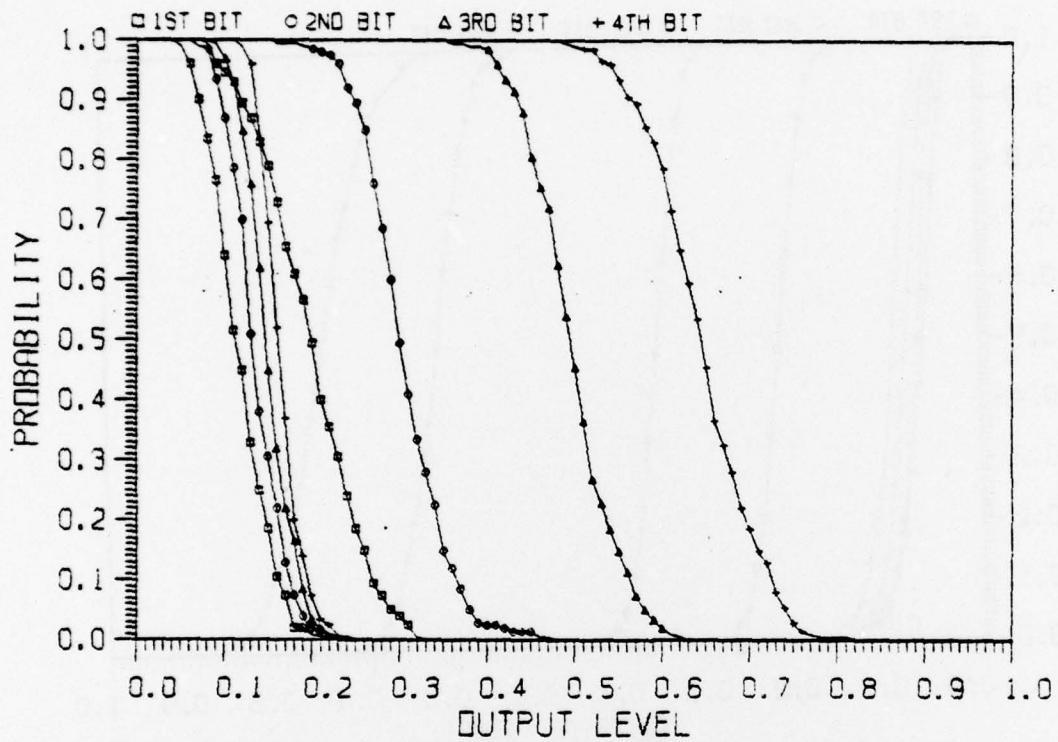


Fig. 6(d) - Probability distribution of Fourier transform filter output
 $\sigma(\text{phase}) = 4$ degrees, $\sigma(\text{amplitude}) = .1$, SNR = 10dB

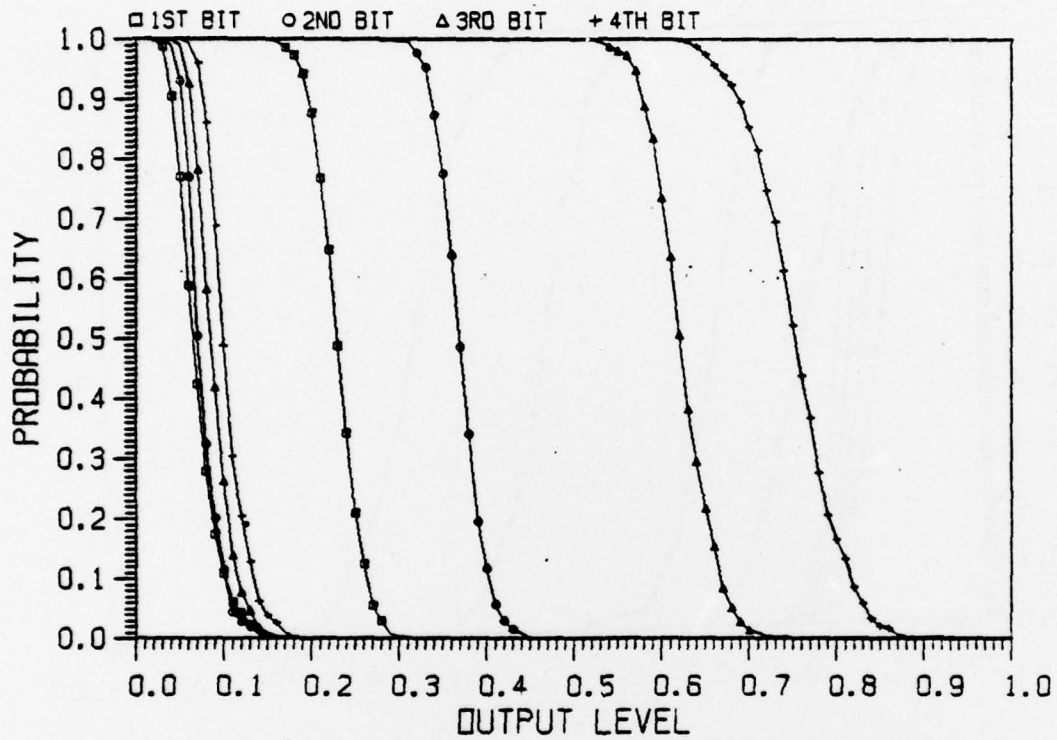


Fig. 7 - Probability distribution of Fourier transform filter output (sum of real and imaginary component) $\sigma(\text{phase}) = 4$ degrees, $\sigma(\text{amplitude}) = .1$, SNR = 20dB